This is the accepted manuscript made available via CHORUS. The article has been published as:

Path differences between quasistatic and fatigue cracks in anisotropic media

Xinyuan Zhai, Thomas Corre, Ataollah Mesgarnejad, Alain Karma, and Véronique Lazarus

Phys. Rev. E **110**, L063001 — Published 13 December 2024

DOI: 10.1103/PhysRevE.110.L063001

Path differences between quasistatic and fatigue cracks in anisotropic media

Xinyuan Zhai,[1] Thomas Corre,[1,2] Ataollah Mesgarnejad,[3] Alain Karma,[3] and Véronique Lazarus[1,*]

[1] *IMSIA, CNRS, EDF, ENSTA Paris, Institut Polytechnique de Paris, 91120 Palaiseau, France*
[2] *Nantes Université, Ecole Centrale Nantes, CNRS, GeM, UMR 6183, F-44000 Nantes, France*
[3] *Physics Department and Center for Interdisciplinary Research on Complex Systems, Northeastern University, Boston, Massachusetts 02115, USA*

(Dated: November 27, 2024)

We report novel experimental observations demonstrating that, in anisotropic media, fatigue cracks under cyclic loading follow strikingly different paths than quasistatic cracks under monotonic loading. We find a qualitatively similar behavior in a computational model, which suggests that this path difference is a general phenomenon. In both experiments and computations, quasistatic cracks follow paths governed by the anisotropy of the fracture energy, as theoretically expected. In contrast, fatigue cracks follow paths predominantly dictated by the symmetry of the loading with the microstructure playing a negligible or subdominant role. Those results pave the way for future studies aimed at elucidating the failure mechanisms underlying this surprising behavior.

Over and above the fascination with the shapes it creates [1], understanding how and when cracks form is of broad importance [2], for instance, in the design of manufacturing processes [3–5], in geophysics for a better understanding of earthquakes [6, 7], in mechanical engineering with obvious societal issues of safety [8, 9]. Cracks or sharp defects are known to particularly affect the resistance to fracture of any material as they lead to stress concentration in their vicinity [10]. The theoretical framework [11–13] and computational tools to predict brittle crack paths in diverse settings, including complex three-dimensional geometries [14–16], are by now well-developed. However, what criterion should be used to predict crack paths is still not fundamentally understood in the practical case of *fatigue* crack growth occurring progressively under a repetitive cyclic load. Such kind of solicitations are common for industrial components (*e.g.,* turbines, rotors, bridges), as well as in earth and life sciences (*e.g.,* waves, tidal ebb and flow, weather or climate cycles, walking/running steps).

To date, it has been commonly assumed that fatigue cracks follow the same path as *quasistatic* cracks that propagate infinitesimally slowly (*i.e.,* at a velocity much smaller than the sound speed) under a monotonic, as opposed to *fatigue* cyclic load [16, 17]. This assumption is based on the qualitative observation that fatigue and quasistatic cracks follow a similar path in *isotropic* materials, *i.e.,* materials with both isotropic elastic properties and a fracture energy independent of the direction of the crack path. In such materials, the principal of local symmetry (PLS) has been traditionally used to predict quasistatic crack paths [11] for 2D plane strain or plane stress within the traditional framework of LEFM; 3D out of plane mode III loading causes crack front segmentation, but the propagation of segmented fronts remains consistent with the PLS [16]. The PLS assumes that the stress distribution remains symmetrical about the instantaneous crack axis during propagation and corresponds to a vanishing mode II stress intensity factor ($K_{II} = 0$). It stems from the fact that cracks with non-vanishing K_{II} kink by a discontinuous change of propagation direction. Therefore, cracks following curvilinear paths, with a continuous change of direction, should propagate with $K_{II} = 0$ [12]. Such crack paths also maximize the energy release rate, *i.e.,*, the rate at which the stored elastic energy in the material is released, taking into account the energy cost Γ (per area) of creating new fracture surfaces. The PLS and Maximum Energy Release Rate (MERR) criteria predict slightly different kink angles [18] for a crack initially loaded with a finite K_{II}, but the same curvilinear paths with $K_{II} = 0$.

For anisotropic materials, the PLS is not applicable but extensions of the MERR criterion have been used to predict crack paths in various contexts [13, 19–22]. A MERR criterion for anisotropic media was formally derived within the diffuse interface phase-field approach to brittle fracture [13, 20] by taking into account the anisotropy of the fracture energy quantified by the function, $\Gamma(\theta)$, where θ is the angle between the instantaneous crack propagation direction and some fixed reference axis. The selected crack path was shown to be the one that maximizes with respect to θ the energy released $G(\theta) - \Gamma(\theta)$, where $G(\theta)$ quantifies the elastic strain energy available by unit surface to propagate the crack in the $\theta-$direction. Consequently, the crack is predicted to propagate with a finite K_{II} proportional to $d\Gamma(\theta)/d\theta$ evaluated about the instantaneous crack axis. This condition reduces to the PLS ($K_{II} = 0$) in isotropic media while, in strongly anisotropic media, it predicts that cracks follow paths that minimize the fracture energy.

The MERR criterion has been validated for quasistatic brittle fracture by phase-field simulations [13, 22] as well as experiments using materials with a composite microstructure engineered to have nearly isotropic elastic properties but a strongly anisotropic fracture energy [22]. However, it is not expected to apply to fatigue cracks that propagate under cyclic loads that peak at $G(\theta)$ magnitudes well below the Griffith threshold $\Gamma(\theta)$; fatigue

cracks do not obey the MERR energy balance condition $G(\theta) = \Gamma(\theta)$, which is valid at each instant of propagation of a quasistatic crack. Fatigue crack growth is more commonly described by a phenomenological Paris-type law $da/dN = C\Delta K_I^n$, which relates the crack advance per cycle to the variation ΔK_I of mode I stress intensity factor during each cycle. Since MERR and Paris criterion have different physical origins, there is no reason to expect that the MERR criterion with $K_{II} \sim d\Gamma(\theta)/d\theta$ is applicable to fatigue crack paths. For fatigue crack growth in isotropic media, the PLS can be rationalized in the same way as for quasistatic fracture by remarking that cracks with $K_{II} \neq 0$ kink, and that therefore smooth cracks should propagate with $K_{II} = 0$. However, it remains largely unknown how fatigue and quasistatic crack paths differ in anisotropic media and, in the absence of a MERR criterion, what physically controls the former.

In this Letter, we address those questions by comparing quasistatic and fatigue crack paths both experimentally and computationally in two model materials where the elastic properties are isotropic, but the fracture energy is strongly anisotropic. We demonstrate that in both cases, quasistatic and fatigue, cracks follow strikingly different paths. The experiments use 3D-printed samples with a criss-cross microstructure yielding a fracture energy $\Gamma(\theta)$ with a strong four-fold anisotropy. As illustrated in Fig. 1, in samples with the same printed structure and loading in pure tensile mode I or with the addition of a shear mode II component, quasistatic cracks follow non-vanishing K_{II} directions corresponding to sharp local minima of the fracture energy, as expected from MERR. In contrast, somewhat surprisingly, fatigue cracks follow vanishing K_{II} directions despite the strong anisotropy of the underlying microstructure. The phase-field computations use a different two-fold anisotropic form of $\Gamma(\theta)$, which was previously used to validate the MERR criterion for quasistatic crack paths in anisotropic media [13, 22]. They yield similar results as the experiments with the difference that fatigue cracks follow paths where K_{II} is much smaller than along quasistatic crack paths, but non-vanishing. This suggests that the path differences between quasistatic and fatigue cracks is a general phenomenon, opening a new avenue of research aimed at a complete understanding of fatigue crack growth in anisotropic media. We describe the experiments and computations in what follows and further interpret our findings.

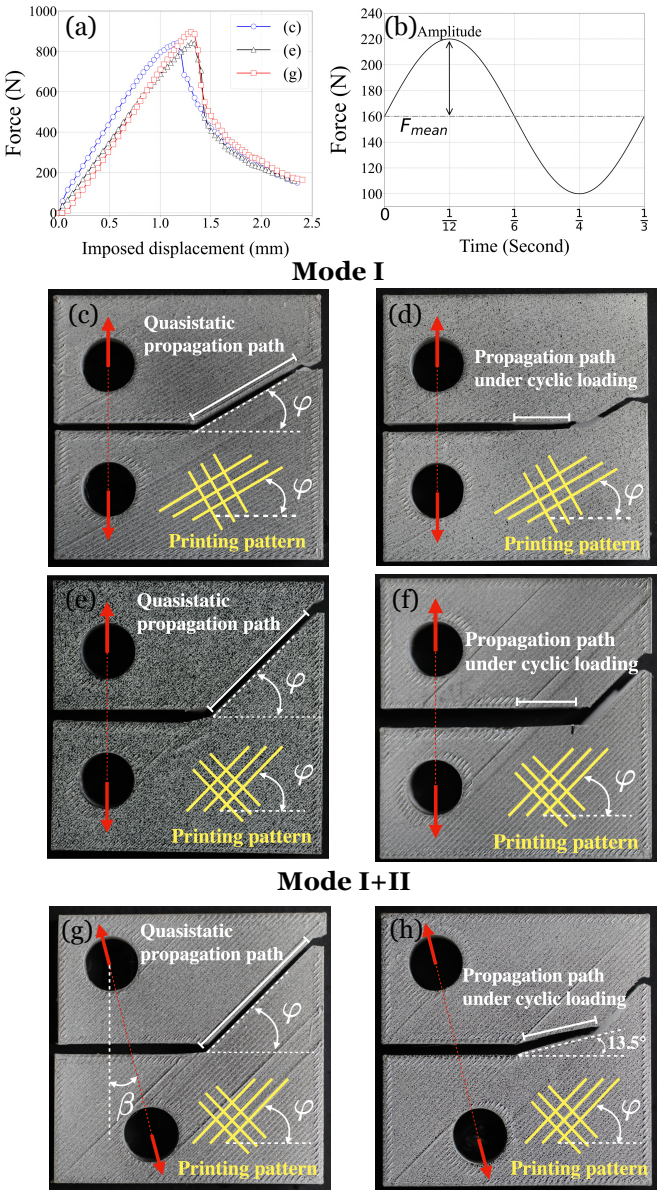


FIG. 1. Different crack propagation paths observed under monotonic load (left column) and cyclic load (right column) in polycarbonate CT (c-f) or CTS (g, h) samples printed by FDM. Under increasing imposed displacement (a), the crack propagates quasistatically in the weak plane of the microstructure (c, e, g) until brutal failure in another direction. Under cyclic load (b), propagation occurs along a different path (d, f, h) during all the fatigue cycles. Bifurcation in the weak plane occurs an increasing load is applied to break the specimen completely. (Samples geometry: $50 \times 48 \times 8$ mm^3. c,d: $\varphi = 30°$; e, f: $\varphi = 45°$;g, h: $\varphi = 45°$, $\beta = 15°$)

To address the question experimentally, polycarbonate Compact Tensile (CT) and Compact Tensile Shear samples (CTS) are printed by Fused Deposition Modeling (FDM) following a 100% filling criss-cross pattern: each successive layer is oriented at 90° to the previous one, with a φ inclination to the initial crack Fig. 1). Tensile tests on samples with different filling angles, showed that the material is nearly isotropic with Young modulus $E \sim 2000$ MPa and Poisson' ratio $\nu = 0.34$ [23]. Once printed, a sharp crack is introduced by fatigue [24], and a black-and-white speckle is applied to the samples prior to testing for Digital Image Correlation (DIC). To propagate the crack, the samples are loaded in a tensile

machine either by increasing monotonically the displacement at a constant rate of 0.5 mm/min for the quasistatic propagation case (Fig. 1a) or by applying a 3 Hz cyclic force load for fatigue (Fig. 1b). In both cases, the crack advance rate is negligible (6-10 mm/min for quasistatic, $4.\,10^{-3} - 10^{-1}$ mm/min for fatigue) compared with the velocity of the elastic wave ($\sqrt{E/\rho} \sim 1200$ m/s), so that no dynamic effect comes into play [25]. While the load is mirror-symmetric to the crack plane for CT samples corresponding to pure mode I, a non-zero β tilt for CTS samples induces non-symmetrical mode I+II loading. Additional technical information on the setup is given in supplemental material [26].

Figure 1 highlights the difference between quasistatic and fatigue propagation on a set of representative cases. Applying increasing displacement, the force-displacement curve has a mountain shape (Fig. 1a). Before the peak, no crack propagation occurs, and the force-displacement curve is quasi-linear, consistent with linear elasticity. After the peak, the crack propagates quasi-statically and the force drops slowly. Fracture occurs in the φ direction (Fig. 1c, e, g) for both CT and CTS. At the microstructure scale, it corresponds to separating two parallel threads on every other layer, and to the orthogonal breaking of the threads on the remaining layers. Applying cyclic loading (Fig. 1b), the crack progressively advances with each loading cycle. The crack advances straight ahead for CT samples (Fig. 1d, f), while a kink is observed for CTS (Fig. 1h) but in a different direction to that obtained under monotonic loading (Fig. 1g). At the microstructure scale, the crack does not generally follow the orientation of the threads. We have performed experiments for different values of β and φ, with good reproducibility and similar differences in the propagation paths. We have also checked by microscopic observation of the crack surfaces and by tomographic imaging, that the evolution of the crack front is uniform in the sample thickness, resulting in a planar fracture surface and rectilinear crack front, and that no major decohesion occurs between the layers. For each case, the crack is oriented by the microstructure for monotonic loading and by the loading orientation for fatigue.

To find out more about the underlying crack propagation rules, and in particular, if the PLS is retrieved in fatigue, the stress intensity factors (K_I, K_{II}) are measured by DIC [23, 27] using the open-source software UFreckels [28, 29]. Figure 2 shows their evolution during crack propagation for the experiments of Fig. 1 (c, d, g, h). For monotonic load and CT samples (Fig. 2a), only mode I builds up before propagation while the applied load is increased; for CTS samples (Fig. 2b), mode I and II contributions increase. This is due to the symmetry and non-symmetry of the CT and CTS setups respectively. At the onset of propagation, the

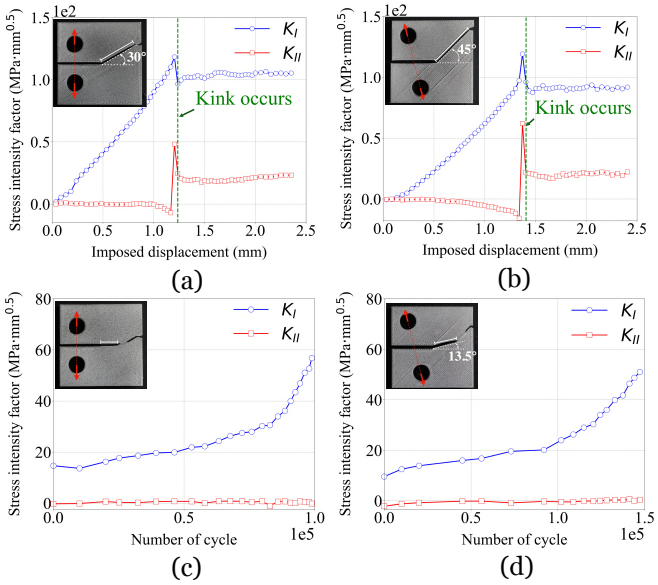


FIG. 2. Evolution of the stress intensity factors during crack propagation measured by DIC. They are measured along the path indicated by a white segment in the insets. $K_{II} \neq 0$ during quasistatic propagation (a, b). $K_{II} = 0$ in both CT and CTS during fatigue propagation (c, d)

quasistatic crack changes direction and a jump in the value of K_I and K_{II} is observed. This jump is consistent with LEFM [18] as demonstrated in [23]. As $K_{II} \neq 0$, the PLS is not verified but the crack propagation direction can be predicted by a MERR criterion as in previous studies of quasistatic crack propagation in anisotropic media [13, 19–22, 24, 26]. For cyclic load (Fig. 2c, d), the crack propagates as soon as cycling begins. The stress intensity factors evolution is the same as that expected for an isotropic material: (i) K_I increases for fixed applied force from the increase of the crack length [30], (ii) $K_{II} = 0$ as soon as the crack propagates in agreement with the Principle of Local Symmetry. In brief, contrary to the quasistatic case, fatigue propagation follows the propagation rules of isotropic material and is not affected by the anisotropy of the microstructure.

To show that the difference between quasistatic and fatigue crack paths in anisotropic media is a general phenomenon and to get further insights, we compute the crack propagation for the two-fold anisotropy [13, 22] $\Gamma(\theta) = \Gamma_{max}\sqrt{\mathcal{A}^{-2}\cos^2(\theta-\phi) + \sin^2(\theta-\phi)}$ where $\mathcal{A} = \Gamma_{max}/\Gamma_0$ measures the toughness ratio for propagation perpendicular to (Γ_{max}) and parallel to (Γ_0) a weak plane analogous to one of the thread axis in the experiments. This form causes quasistatic cracks to follow directions close to weak planes for sufficiently strong anisotropy [13, 22]. Quasistatic propagation was modeled using

the well-established alternate minimization scheme applied to anisotropic media in [22]. Fatigue crack growth was investigated using a recently developed phase-field model of fatigue [31] that enables crack growth below the Griffith threshold ($G < \Gamma$) by degradation of the fracture toughness [32]. This formulation has reproduced salient features of fatigue crack growth, such as the Paris law and non-trivial 2D and 3D crack paths in isotropic media [31]. We simulate a compact specimen of width W [33]. Details of the numerical methods are given in the supplementary material [26]. The loading is applied via a vertical displacement u_y on the top half of the upper hole and by setting $u_x = u_y = 0$ around the lower hole. In this geometry, the energy release rate decreases for displacement-controlled loading as the crack propagates. Therefore, in both quasi-static and fatigue simulations, we set the displacement $u_y = k\ell$ where $\ell = 2\sqrt{\Gamma_{max} W/3E} = 3EK_{IC}^{max}\sqrt{3W}/2$ and slowly increase k such that quasi-static crack propagation remains energetically stable and fatigue cracks are able to propagate an extended distance. For quasi-static propagation, we vary k from 0 to 4. The onset of crack propagation occurs at $k \approx 1.6$ and $k \approx 2.6$ for $\phi = 30°$ and $\phi = 90°$, respectively, followed by quasi-static crack propagation when k is increased above these thresholds. For fatigue, we set $k = 1.5$ for $\phi = 90°$ below its quasi-static limit. We increase k from 1 to 2.25 for $\phi = 30°$, which ensures that the energy release rate at the crack tip remains at all times above the minimum threshold G_{min} for fatigue crack growth but below the Griffith threshold $G = \Gamma$ for quasi-static propagation. Further details of the phase-field methods can be found in [22] for quasi-static and [31] for fatigue crack propagation.

The results are shown in Fig. 3 which compares quasistatic and fatigue crack paths for a large anisotropy $\mathcal{A} = 4$ and two different weak plane orientations. When the weak plane is perpendicular to the horizontal axis (left panel of Fig. 3 for $\phi = 90°$), the quasistatic crack kinks at a large angle to follow a direction close to the weak plane with $K_{II} \neq 0$. In contrast, the fatigue crack propagates straight with $K_{II} = 0$. When the weak plane is at a 30° angle with respect to the horizontal axis (right panel of Fig. 3 for $\phi = 30°$), the quasistatic crack kinks to follow again a direction close to the weak plane, while the fatigue crack is much more weakly defected to propagate in a direction with K_{II} much smaller than the quasistatic crack, but non-vanishing. We note that, here, the computational $\phi = 90°$ case mimics the $\phi = 45°$ experimental case with pure tensile loading. This is because the fracture energy is two-fold and four-fold in the computations and the experiments, respectively, so both cases are mirror symmetric about the horizontal axis. In contrast, the $\phi = 30°$ cases break this symmetry in both the computations and the experiments.

From a general symmetry viewpoint, we would expect fatigue cracks to follow a direction that is influenced both by the symmetry of the loading, which dictates a preferential axis for the cyclic damage process (*e.g.,* the principal stress axis), and the symmetry of the underlying microstructure of the material, which offers the possibility for damage to occur preferentially in certain directions (*e.g.,* parallel to the thread axis). The experiments demonstrate that the symmetry of the loading plays a dominant role in the printed materials investigated here. Under pure tensile loading, the stress fields are mirror-symmetric about the horizontal propagation axis, and fatigue cracks propagate along this axis. They follow the PLS irrespective of the orientation of the microstructure (*i.e.,* $\varphi = 45°$ and $\varphi = 30°$ yield identical fatigue crack paths with $K_{II} \approx 0$, Fig. 1d, f). In contrast, in the computations, the symmetry of the microstructure plays a subdominant, albeit not entirely negligible, role. For $\phi = 90°$, both the loading and the microstructure (*i.e.,* $\Gamma(\theta)$) are mirror-symmetric about the horizontal axis, and the fatigue crack propagates straight with $K_{II} = 0$. For $\phi = 30°$, the microstructure is no longer mirror-symmetric about the horizontal axis, thereby causing the fatigue crack to propagate at a small angle. The experimental and computational observations presented here demonstrate that quasistatic and fatigue crack paths can be strikingly different. They further demonstrate that loading plays a dominant role in two model cases where quasistatic crack paths are largely dictated by the microstructure. Further studies are warranted to elucidate the relative importance of loading and microstructure in dictating fatigue crack paths. These results also appeal for similar studies to determine the degree of generality, in particular how they extend to other anisotropic materials: additive manufacturing [5] plastic, ceramics or metals [34], single crystals [35, 36] as those used in some photovoltaic or aerospace turbine blades, natural materials as rocks, clay, bones, wood [37, 38] and composite materials [22, 39], in particular cross-ply composites whose microstructure is close to the system studied here [40]. We believe that further study of fatigue in anisotropic materials can also help to gain a deeper physical understanding of fatigue crack propagation, which is still lacking even for isotropic materials.

The research at Northeastern University was supported by the United States NSF-CMMT grant 1827343. The research at ENSTA Paris was partially supported by Agence de l'Innovation de Défense – AID - via Centre Interdisciplinaire d'Etudes pour la Défense et la Sécurité – CIEDS (AID-2018 60 0071 00 470 75 01 and FracAddi project 2022), by Agence Nationale de la Recherche (ANR-23-CE51-0054) and by IP Paris Doctoral Allocation. The authors thanks N. Thurieau, L. Cherfa for their help in the experiments.

For the purpose of Open Access, a CC-BY public copyright licence (`https://creativecommons.org/licenses/by/4.0/`) has been applied by the authors to

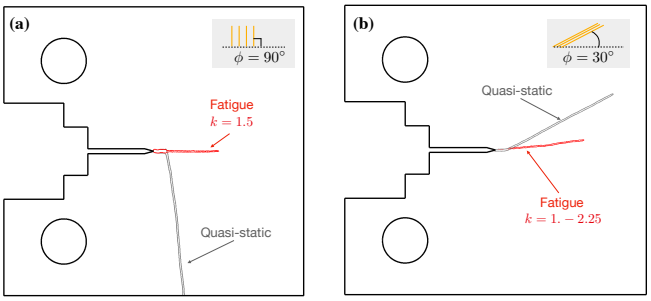


FIG. 3. Comparison of computed quasi-static (gray) and fatigue (red) crack paths with the weak plane at (a) $\phi = 90°$ (b) $\phi = 30°$ with respect to the horizontal propagation axis.

the present document and will be applied to all subsequent versions up to the Author Accepted Manuscript arising from this submission.

* veronique.lazarus@ensta-paris.fr

[1] D. Hull, *Fractography*, edited by C. U. Press (Press syndicate of the university of Cambridge, UK, 1999).
[2] B. Cotterell, *Fracture And Life* (Imperial College Press, 2010).
[3] K. H. Nam, I. H. Park, and S. H. Ko, Nature **485**, 221 (2012).
[4] V. Lazarus, EPL (Europhysics Letters) **117**, 24002 (2017).
[5] T. D. Ngo, A. Kashani, G. Imbalzano, K. T. Nguyen, and D. Hui, Composites Part B: Engineering **143**, 172 (2018).
[6] S. Fliss, H. S. Bhat, R. Dmowska, and J. R. Rice, Journal of Geophysical Research: Solid Earth **110**, 10.1029/2004JB003368 (2005).
[7] V. Rubino, N. Lapusta, and A. Rosakis, Nature **606**, 922 (2022).
[8] T. L. Anderson, *Fracture Mechanics* (CRC Press, Boca Raton, FL, 2005).
[9] J. Besson, J. Bleyer, S. Feld-Payet, A.-F. Gourgues-Lorenzon, F. Hannard, T. Helfer, J. Hure, D. Kondo, V. Lazarus, C. Le Bourlot, H. Maitournam, C. Maurini, N. Moes, T. Morgeneyer, L. Morin, T. Petit, and A. Simar, *MEALOR II Damage Mechanics and Local Approach to Fracture* (Zenodo, 2023).
[10] M. L. Williams, Journal of Applied Mechanics **19**, 526 (1952).
[11] R. V. Goldstein and R. L. Salganik, International Journal of Fracture **10**, 507 (1974).
[12] B. Cotterell and J. R. Rice, International Journal of Fracture **16**, 155 (1980).
[13] V. Hakim and A. Karma, Journal of the Mechanics and Physics of Solids **57**, 342 (2009).
[14] B. Bourdin, G. A. Francfort, and J.-J. Marigo, Journal of Elasticity **91**, 5 (2008).
[15] B. Bourdin, J.-J. Marigo, C. Maurini, and P. Sicsic, Physical Review Letters **112**, 014301 (2014).
[16] C.-H. Chen, T. Cambonie, V. Lazarus, M. Nicoli, A. J. Pons, and A. Karma, Physical Review Letters **115**, 265503 (2015).
[17] F.-G. Buchholz, A. Chergui, and H. A. Richard, Engineering Fracture Mechanics **71**, 455 (2004).
[18] M. Amestoy and J.-B. Leblond, International Journal of Solids and Structures **29**, 465 (1992).
[19] M. Marder, Europhysics Letters **66**, 364 (2004), publisher: IOP Publishing.
[20] V. Hakim and A. Karma, Physical Review Letters **95**, 235501 (2005), arXiv: cond-mat/0412775 Publisher: American Physical Society.
[21] A. Takei, B. Roman, J. Bico, E. Hamm, and F. Melo, Phys. Rev. Lett. **110**, 144301 (2013).
[22] A. Mesgarnejad, C. Pan, R. M. Erb, S. J. Shefelbine, and A. Karma, Physical Review E **102**, 013004 (2020).
[23] T. Corre and V. Lazarus, International Journal of Fracture **230**, 19 (2021).
[24] X. Zhai, *Crack propagation in elastic media with anisotropic fracture toughness : experiments and numerical modeling*, Ph.D. thesis, Institut Polytechnique de Paris. `https://hal.science/tel-04528865v1` (2023).
[25] L. B. Freund, *Dynamic fracture mechanics*, edited by G. K. Batchelor, C. Wunsch, and J. Rice (Cambridge University press, 1998).
[26] See Supplemental Material at [URL will be inserted by publisher] for Complements about the MERR criterion and Details of the numerical methods.
[27] R. Hamam, F. Hild, and S. Roux, Strain **43**, 181 (2007).
[28] J. Réthoré, International Journal for Numerical Methods in Engineering **103**, 516 (2015).
[29] J. Réthoré, UFreckles v2.0 , 10.5281/zenodo.1433776 (2018).
[30] H. Tada, P. C. Paris, and G. R. Irwin, *The Stress Analysis of Cracks Handbook*, edited by T. A. S. of Mechanical Engineers (Professional Engineering Publishing, 2000).
[31] B. E. Grossman-Ponemon, A. Mesgarnejad, and A. Karma, Engineering Fracture Mechanics **264**, 108255 (2022).
[32] A. Mesgarnejad, A. Imanian, and A. Karma, Theoretical and Applied Fracture Mechanics **103**, 102282 (2019).
[33] ASTM, *Standard Test Method for 1 Measurement of Fracture Toughness*, Tech. Rep. E 1820-05 (ASTM).
[34] D. Roucou, T. Corre, G. Rolland, and V. Lazarus, Materials Science and Engineering: A **878**, 145176 (2023).
[35] R. Deegan, S. Chheda, L. Patel, M. Marder, H. Swinney, J. Kim, and A. de Lozanne, PHYSICAL REVIEW E **67**, 10.1103/PhysRevE.67.066209 (2003).
[36] S. Nagaraja, P. Carrara, and L. De Lorenzis, Engineering Fracture Mechanics **293**, 109684 (2023).
[37] M. Nejati, A. Aminzadeh, F. Amann, M. O. Saar, and T. Driesner, International Journal of Solids and Structures **195**, 74 (2020).
[38] L. Goehring, A. Nakahara, T. Dutta, S. Kitsunezaki, and S. Tarafdar, *Desiccation cracks and their patterns: Formation and modelling in Science and Nature* (Wiley, 2015).
[39] P. O. Judt, J.-C. Zarges, A. Ricoeur, and H.-P. Heim, Engineering Fracture Mechanics **188**, 344 (2018).
[40] R. F. Teixeira, S. T. Pinho, and P. Robinson, Composites Part A: Applied Science and Manufacturing **90**, 33 (2016).